

# Explainable AI (XAI) for Wireless Communications: UWB Radar for Zone-based Obstacle Detection

Mohammad Cheraghinia, Eli De Poorter, and Adnan Shahid, *Senior Member, IEEE*

**Abstract**—The evolution of artificial intelligence (AI) solutions in various fields has raised concerns about managing and understanding these solutions. Ultra-wideband (UWB) radar, known for its precision and reliability, is extensively applied in localization scenarios. However, the increasing use of AI in this field has led to concerns regarding the ambiguity of analytical reasoning in AI solutions. To address these concerns, XAI has been introduced to make these solutions more trustworthy and understandable. This study explores the integration of XAI within UWB radar technology, emphasizing the identification of target zones through zone-based obstacle detection. We investigate the integrated gradient method and its application in a convolutional neural network (CNN) model. A significant portion of the study is dedicated to analyzing the distance and angle for zone-based obstacle detection facilitated by the XAI-empowered CNN model. This analysis aims to provide deep insights into the reasoning mechanics of AI solutions in UWB radar technology, thereby addressing concerns in the field.

**Index Terms**—UWB Radar, Machine Learning (ML), Explainable Artificial Intelligence (XAI), Angle of Arrival (AOA), Localization, Integrated Gradients

## I. INTRODUCTION

AI has appeared across various sectors, revolutionizing many aspects of technology. However, it has also raised concerns regarding the interpretability and transparency of AI-driven solutions. Explainable Artificial Intelligence (XAI) is proposed as a solution to improve understandability and trust in such wireless applications by focusing on clear explanations, allowing a better understanding of which input features are used by the neural network, which potential bias or generalizability problems might occur, and providing a better understanding of why the solution outperforms traditional algorithms.

The main focus of this paper is to address the need for more transparency and clarity in AI-driven communication systems. It explores the application of one XAI method (“integrated gradients”) in CNN models. As a typical example of a wireless technology that increasingly relies on AI techniques, we will consider UWB radar technology, which often uses neural networks for tasks such as Angle of Arrival (AOA) estimation, distance estimation, and activity recognition. While AI-based AOA estimation in UWB [1] demonstrates superior performance compared to traditional benchmarks like MUSIC [2]

and PDOA [3], these AI solutions lack explicit explainability and interpretability and are often treated as “black boxes,” not providing any motivation on why their performance is better, nor explaining which boundary conditions might arise that negate the improved performance of the used neural networks.

The main contributions of this paper are as follows:

- Investigate the integration of XAI, particularly integrated gradients, for AOA estimation and distance estimation in UWB radar systems.
- Design and develop an XAI-empowered CNN model for AOA estimation and distance estimation.
- Provide a detailed analysis of distance and angle classifications facilitated by the XAI-empowered CNN model, offering insights into AI decision-making.

The paper is structured as follows: First, Section II provides an overview of related work. Next, Section III delves into the system model, presenting UWB radar technology and an overview of AOA and distance estimation methods. Section IV discusses the experimental setup and dataset, providing insights into the practical aspects of the research and the data used for model training and testing. Section V elaborates on the methodology, including the explanation of integrated gradients and the proposed CNN for classifying the radar data. Section VI presents the results, highlighting the findings from applying the CNN model to distance and AOA classification for zone-based obstacle detection and the insights gained through XAI. Finally, Section VII concludes the paper by summarizing the key findings, discussing the implications of the research, and suggesting directions for future work in the field of UWB radar and AI.

## II. RELATED WORKS

### A. UWB Radar for AOA and Distance Estimation

Whereas AOA estimation is well-studied for determining the angle of tags that transmit signals, tag-free angle estimation of persons or objects using UWB radar is less studied. A noteworthy exception is the study conducted by Hong et al. [4]. This paper proposes a two-stage learning-based method employing a single-antenna transmitter and multi-antenna receivers. This approach achieved Root Mean Square Errors (RMSEs) of 7.13 and 6.61 degrees for 4 and 8 antenna scenarios, demonstrating the method’s efficacy.

Prior work is more common for UWB tag-free distance estimation of humans or obstacles using UWB radar. [5] demonstrates how selecting data processing methods and

The authors, M. Cheraghinia, E. De Poorter, and A. Shahid, are affiliated with IDLab, Department of Information Technology, Ghent University - imec, 9052 Ghent, Belgium. Emails: (Mohammad.Cheraghinia, Eli.DePoorter, Adnan.Shahid)@UGent.be.

distance estimation techniques (mean- and variance-based) influences the detection accuracy of low-cost DW1000 UWB transceivers. [6] develops an IR-UWB distributed MIMO radar system that supports multi-object localization and vital sign monitoring, demonstrating an advantage over existing methods. [7] presents a UWB device-free person recognition and range technique that performed well in a variety of scenarios while also admitting potential concerns with outliers. [8] creates a multi-static radar network that demonstrates promise for IoT applications despite issues with low signal-to-noise ratios and range specifications. [9] unveils a novel approach to Device-free Localization that leverages UWB channel impulse responses, delivering improved accuracy. [10] studies the capabilities of UWB radar for detecting static humans behind various wall materials, employing Singular Value Decomposition (SVD) and Wavelet Transform to improve distance estimate, particularly with low dielectric wall materials.

The works showcase the potential uses and difficulties of utilizing UWB radar systems to measure distance and angle. However, they need to consider the antenna's significance and the specific areas of the Channel Impulse Response (CIR) that contain the necessary information for their models, should they be using AI. Our work delves into the reasoning behind the AI model in depth.

### B. XAI Approaches in Related Applications

The utilization of XAI to interpret complicated sensor data is a recent research trend aiming to improve awareness of model predictions and the importance of their features. As an illustration, [11] addresses fall detection systems utilizing a multi-sensor method and Local Interpretable Model-Agnostic Explanations (LIME). This work uses XAI to optimize sensor location and comprehend temporal sensor patterns. Similarly, [12] uses a deep learning network for real-time occupancy identification using WiFi sensing, with the Grad-CAM algorithm used to assess feature significance, demonstrating the relative insignificance of certain ambient input parameters such as humidity and temperature. A third example of XAI is used to analyze sleep stages. [13] uses an attention-based technique combined with bidirectional LSTM and IR-UWB radar to understand the input sensors' interpretation better.

Our review has shown that no studies have utilized Integrated Gradients to improve the interpretability of models in this area. Furthermore, we have discovered that no previous research has applied XAI principles to analyze AOA and distance in the context of UWB radar systems. This gap presents a chance for our XAI approach to shape future research directions.

## III. SYSTEM MODEL

This section will provide a concise overview of UWB radar fundamentals and discuss how this technology enables angle and distance estimation.

### A. Introduction to UWB radar technology

We consider a UWB radar setup to consist of a transmitter sending a signal, which is reflected by both the environment and one or more objects of interest. The reflected signal is received by a secondary receiver with one or more antennas.

UWB technology is distinguished by its capability to spread data across a broad frequency band via short pulses, with a higher tolerance to multipath interference than narrowband signals. The UWB radar received signal known as CIR can be modeled as follows [14], [15]:

$$CIR(t) = \sum_{i=1}^L A_i \delta(t - \tau_i) + \nu(t) \quad (1)$$

where  $A_i$  represents the amplitude of the  $l_{th}$  path,  $\tau_i$  is the time of the delay,  $\delta(t - \tau_i)$  is the received pulse, and  $\nu(t)$  is the noise. Due to its complex representation, the CIR sample captures not only the intensity (amplitude) but also the arrival timing (phase) of each reflected path, enabling a thorough understanding of the received signal.

### B. Overview of AOA and distance estimation methods

Based on the received signal, the distance to and the angle of the object of interest can be estimated relative to the receiver.

1) *AOA estimation*: To effectively implement AOA estimation, it is necessary to have at least two antennas; however, more antennas can be used to enhance accuracy and resolution. The phase difference between these antennas, which captures the time displacement between received signals, is the main component used for accurately determining the direction of an incoming signal. A common technique to determine the angle of arrival of a signal at a receiver is PDOA. The angle  $\theta$  can be calculated using the following equation:

$$\theta = \arcsin\left(\frac{\alpha\lambda}{2\pi d}\right) \quad (2)$$

where  $\alpha$ ,  $\lambda$ , and  $d$  represent the phase difference of arrival, the wavelength of the signal, and the distance between the antennas, respectively.

2) *Distance estimation*: Various distance estimate methods, such as clutter subtraction, target detection, and target localization procedures, are extensively used in UWB radar systems. If we assume that a CIR is received in an environment that is free from clutter and noise, we can use the following formula to calculate the distance of the target from the setup:

$$Dist = (c \times (TR - FP))/2 \quad (3)$$

where  $TR - FP$  represents the round-trip time (RTT), which is the total time it takes for the transmitted signal to travel to the target, reflect off it, and return to the receiver. Dividing this value by two gives us the one-way travel time. In this equation,  $TR$  is the target reflection time stamp,  $FP$  is the first path time stamp received from the transmitter, and  $c$  is the speed of the signal, which is approximately  $3 \times 10^8$  m/s.

In cluttered environments, clutter subtraction uses advanced signal processing methods to reduce the impact of unwanted reflections or clutter in received signals. This allows for the

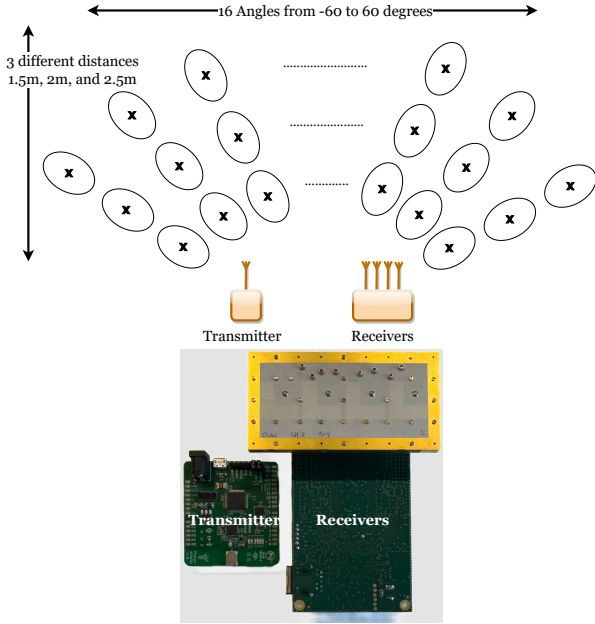


Fig. 1: UWB setup for zone-based obstacle detection. Each zone X corresponds to a sampling point. A transmitter with a single antenna is used, and a receiver with 4 antennas. The object of interest in the zone consists of a metallic pipe.

extraction of appropriate target signals and improves distance estimate accuracy. Target detection methods entail recognizing and isolating possible target objects in radar data, often via the use of thresholding or statistical analysis techniques. Finally, target localization algorithms determine the precise location or position of the target using the observed time-of-flight (ToF) of the UWB signals. These distance estimate algorithms work together to provide precise and dependable range and localization in UWB radar systems.

#### IV. EXPERIMENTAL SETUP AND DATASET

In our UWB radar experiment, we focus on detecting the zone of presence of an obstacle (metallic pipe (22×8×150cm)) based on the target’s location. The radar setup incorporates two essential components: a transmitter and four receivers, similar to the setup from [1] where AOA was investigated in a non-radar, tag-based setup. The configuration, depicted in Fig. 1, involves employing a DW1000 with an integrated chip antenna as the transmitter device responsible for emitting radar signals. On the other hand, the receiver device consists of a board housing four DW1000 chips designed to capture and process the reflected signals transmitted by the transmitter. A separation distance of 75 cm between the devices is chosen to achieve precise and controlled radar signal transmission. In this experiment, the radar system operates on channel 7 of the UWB standard, utilizing a center frequency of 6.49 GHz and a bandwidth of 1.08 GHz.

To simulate an industrial environment resembling a warehouse with metallic objects, the dataset is captured in the Industrial IoT Lab in UGent IDLab [16], representing a realistic warehouse environment consisting of an open area surrounded by walls and metallic racks. A metallic galvanized

cubic tube is positioned at three distances from the radar setup: 1.5m, 2m, and 2.5m. Additionally, the tube is set at 16 different angles, ranging from -60 to 60 degrees. This configuration facilitates the capture of a comprehensive dataset encompassing 48 possible zones for the obstacle (3 distances, 16 angles). Considering varying distances and angles, this dataset provides insights into the interaction between the radar signals and the metallic target.

The captured data are CIR samples with real and imaginary parts with the size of 1000 samples in each experiment; however, to simplify the training process, we only used 100 samples to improve the visualizations. In our dataset, we calculate the respective amplitude and phase of the CIR samples as data points for each of the four antennas. As a result, we can have two data types, one based on the amplitude and the other based on the phase of the CIR samples. Each of these amplitudes and phases has the exact size of the CIR sample and can be directly incorporated into the same CNN model.

#### V. XAI METHODOLOGY

##### A. Integrated gradients

Integrated Gradients [17] is designed to attribute importance to the individual features of deep neural networks, providing feedback about which input features are most used by the neural network. The core idea involves comparing the model’s prediction for an actual input against a predefined baseline (denoted as  $x'$ ), which represents the absence or neutral state of input features. To this end, it satisfies the sensitivity and implementation of invariance axioms, ensuring meaningful attributions.

Let  $IG_i(x)$  denote the Integrated Gradient for the  $i$ -th feature of input  $x$ . This computation combines several elements. Firstly, the input feature  $x_i$  corresponds to the value of the  $i$ -th feature in the input data. Alongside this, the baseline feature  $x'_i$  is defined as the value of the  $i$ -th feature when it is in a neutral or absent state, serving as a point of reference or baseline for comparison. The process also involves calculating a path integral, integrating gradients along a direct path from this baseline state  $x'$  to the actual input  $x$ , which is scaled using  $\alpha$  from baseline to input. This path integral, calculated for the  $i$ -th feature, captures how changes in the feature’s value influence the model’s output, providing a detailed attribution of the feature’s importance. The function  $F$  refers to the neural network model being analyzed. The formula for  $IG_i(x)$  is expressed as:

$$IG_i(x) = (x_i - x'_i) \times \int_0^1 \frac{\partial x_i}{\partial F(x' + \alpha(x - x'))} d\alpha. \quad (4)$$

Due to computational limitations, a practical approximation is employed for  $m$  number of steps, and larger steps result in a finer approximation in the below equation:

$$IG_i^{\text{approx}}(x) = (x_i - x'_i) \times \sum_{k=1}^m \left( \frac{\partial x_i}{\partial F(x' + \frac{k}{m}(x - x'))} \right) \times \frac{1}{m}. \quad (5)$$

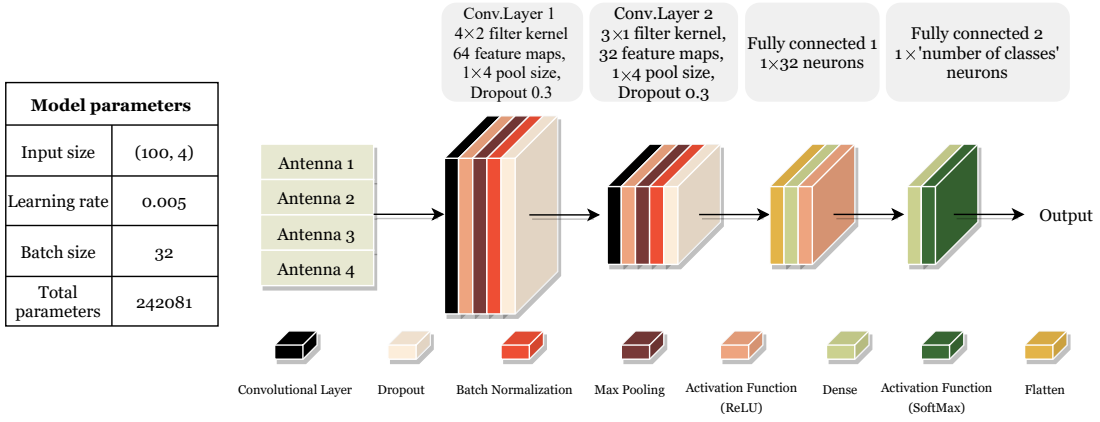


Fig. 2: CNN model for Angle and distance-based zone classification

This approach uses a finite number of steps, typically between 20 to 300, to calculate the sum of gradients. This enables a proper allocation of input features to the model's output. As explained in [17], in our study, the baseline  $x'$  is a zero vector of the same size as the input. The input  $x$  refers to the amplitudes or phases of the CIR samples that serve as the input for the CNN model. The CNN model is further explained in the following subsection and is represented by  $F$  in (4) and (5).

### B. Proposed CNN model

In this study, we use a CNN model shown in Fig. 2 to classify the angle and distance in our dataset separately to determine the zone of the object of interest. The architecture of the selected model is derived through hyperparameter tuning, designed to enhance its performance for this particular task. The input shape of the model is established as  $(100, x)$ , where 100 signifies the length of the CIR sample for each antenna. The value of  $x$  varies according to the attributes chosen from the dataset. For instance, if only the phase or amplitude from each of the four antennas is used, then  $x$  will be 4, reflecting the four attributes from the four receivers in our setup.

Conversely, when both phase and amplitude are utilized for training to evaluate their significance using XAI, the value of  $x$  becomes 8. By setting the input shape to  $(100, x)$ , the data is reformatted into a 2-dimensional array, conforming to the spatial requirements that the CNN model necessitates. This allows CNN to learn and efficiently predict classification based on the discerned features and patterns.

## VI. RESULTS

Here, we analyze both the performance of zone-based obstacle detection and use XAI to explain and understand the inner workings and limitations of the trained neural network. The zone estimation consists of two steps: distance estimation and angle estimation.

### A. XAI-Based Distance Classification

This section is focused on classification outcomes for distance estimation using the CNN from Section IV using

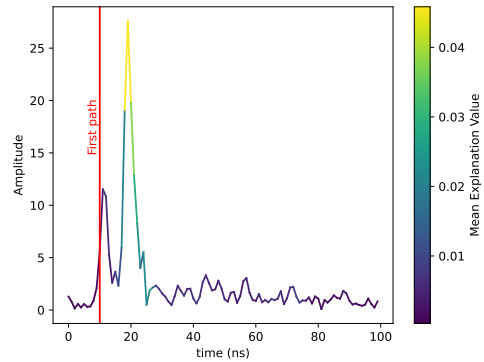


Fig. 3: Sample visualization of integrated gradients to color-code AOA classifications in a CIR sample taken 1.5m away from the setup. In Fig. 4, each antenna is represented by a column filled with these color-coded explanations. In each experiment, four antennae are used.

different CIR inputs (Amplitude, Phase, or both). We use XAI to analyze the importance of the input features. To this end, Fig. 3 depicts an example of one of the CIR samples where the color is depicted on the CIR. Each column of this visualization represents a color code of the importance of each time sample. Fig. 4 visually displays the integrated gradients for all three input features. For instance, We note the following observations:

**Observation 1: For distance estimation, the integrated gradients for the amplitude data are much more focused than the ones from the phase information.** Fig. 4a demonstrates that the amplitude information focuses clearly on the CIR peak corresponding to the correct distance. For the phase information Fig. 4b, the input features focus on a broad range of CIR peaks, resulting in less clear identification of the correct distance. Finally, Fig. 4c shows that adding both input features results in a mixture of both behaviors.

The improved focus of the CNN for amplitude data is confirmed by the actual classification results in TABLE I. The classification accuracies obtained from the CNN model indicate the importance of CIR amplitude, with a remarkable

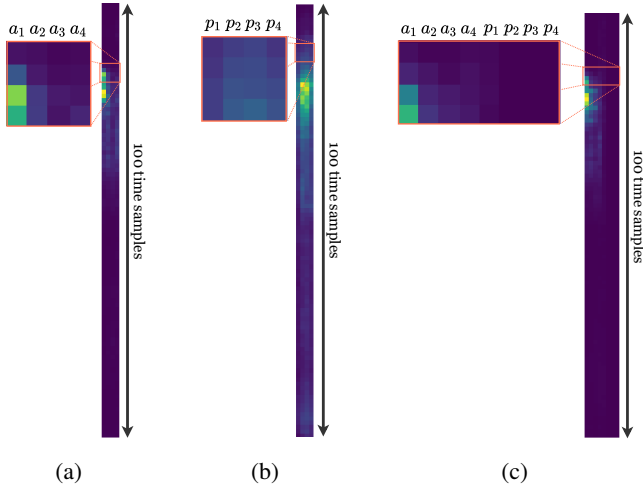


Fig. 4: Integrated gradients for 400 random samples tested in the trained model for distance classification, a) XAI Amplitude information, b) XAI Phase information, c) XAI using amplitude and phase information.

TABLE I: Distance classification test accuracy of the CNN for different input features: Amplitude, Phase, or both.

Amplitude	Phase	Amplitude + Phase
99%	94%	93%

accuracy rate of 99%, as opposed to the phase’s accuracy of 94%. Furthermore, we conducted experiments using both amplitude and phase information as input. Surprisingly, this combined data achieved a lower accuracy rate of approximately 93%, suggesting that including phase data does not provide substantial additional information and actually complicates learning distance patterns.

*Observation 2:* The XAI analysis reveals a further observation: **distance calculations based on amplitude primarily focus on only a single antenna, specifically the one closest to the transmitter** Fig. 4a. This stands in contrast to the behavior of phase-based computations, which demonstrate less precise regions of significance in XAI visualizations, as depicted in Fig.4a and Fig.4b. This result makes intuitive sense since the distance from the transmitter to the reflector and back to the receiver will be the shortest for this antenna, resulting in less signal degradation and less errors due to the increased distance between sender and receiver. On the other hand, the phase-based results include a range of noise and possible reflectors, along with important information, including the reflection from the target.

1) *Lessons learned* : Several lessons were extracted from applying XAI to distance classification in a UWB radar setup. First, experimental results strongly confirm the superiority of amplitude over phase for accurate distance measurement and emphasize the effectiveness of a single, closest antenna. Additionally, joint analysis of amplitude and phase data demonstrated the CNN model’s primary reliance on amplitude, highlighting the low influence of phase, as clearly shown in Fig. 4c. As such, the XAI-based optimization approach pro-

TABLE II: AOA classification test accuracy based on the distance of the target

Distance (m)	Amplitude + Phase	Amplitude	Phase
1.5	99%	98.4%	65.51%
2	97.1%	96.33%	62%
2.5	95.2%	94.4%	61%

vides valuable insights indicating distance estimation solutions should minimize the input features to the CNN to include only amplitude information from the first antenna.

### B. XAI-Based AOA Classification

This section uses the same structure as the previous section, but this time focuses on AOA classification. Fig. 5 visually shows the importance of the different input features using the integrated gradients XAI method, whereas TABLE II shows the actual accuracies.

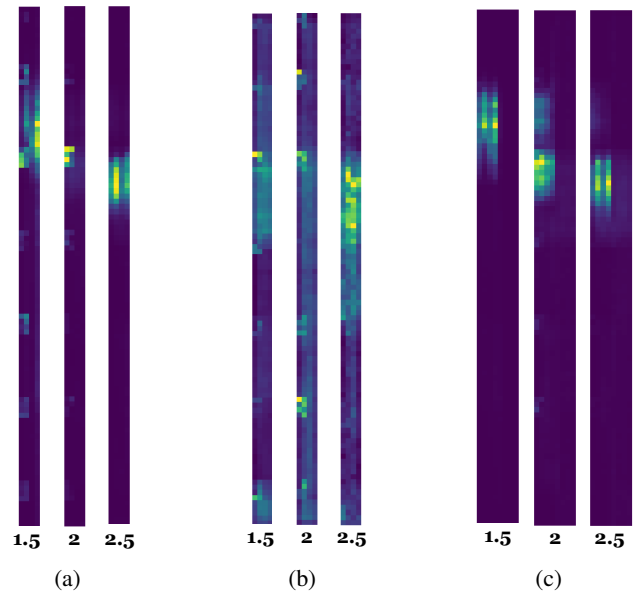


Fig. 5: XAI results for AOA classification at three distances using amplitude, phase, and joint amplitude and phase., a) XAI Amplitude information, b) XAI Phase information, c) XAI using amplitude and phase information.

*Observation 3:* As shown in Fig. 5 **AOA using CNNs rely on information from all four antennas.**, This is in stark contrast with the distance information, where a single antenna was used for input. This makes intuitive sense since a single antenna can not differentiate between different angles. However, it also indicates that the CNN utilizes all four antennas, in contrast to PDOA methods that use the phase difference between only two antennas. As such, this fact is a likely explanation for the improved accuracy obtained by many ML-based AOA estimators in scientific literature, such as the one reported in [1].

*Observation 4:* **For AOA classification, the amplitude CIR input shows much more focused regions (and is hence more reliable) than phase input for angle classification.**

This higher focus density is visible both when using amplitude only Fig. 5a and when using the combination of amplitude and phase Fig. 5c, compared to a diffuse input relevance from Fig. 5b. This seems to indicate that the amplitude information is more relevant for angle estimation than the phase information. This result might be surprising since traditional methods such as PDOA utilize mainly phase information as input. However, the results, shown in TABLE II, confirm that a method using amplitude, analyzed through a CNN, leads to better accuracy in determining AOA. Specifically, the amplitude-based approach was around 33% more precise than phase analysis, particularly when measuring AOA at different distances. This finding suggests that amplitude could be a more accurate factor for AOA zone classification in UWB systems. This has the important implication that the zone recognition most likely focuses on creating a specific lookup table, linking specific amplitude values from all four antennas to a specific zone, which might be an indication that the CNN would not generalize well in new environments.

*Observation 5:* The AOA classification in UWB radar systems, as reflected in the data from Table II, confirms that **AOA classification accuracy decreases with increased distance between the radar and the target object**. The accuracy decreased consistently across different data types—Amplitude + Phase, Amplitude alone, and Phase alone—as the target’s distance extended from 1.5 m to 2.5 m. This reduction in accuracy is likely due to the weakening of the reflection signal strength over longer distances. These results demonstrate the negative correlation between the accuracy of AOA classification and the target’s distance in UWB radar systems. In the UWB radar setup, the CNN model’s approach to AOA classification primarily focuses on target reflections from a distance, incorporating data from all four antennas. The study of CIR samples at different distances shows that in the UWB radar system, the initial reflection from the transmitter remains consistent, but the later reflections, which are specific to the target, change and become delayed as the distance increases. This requires the CNN model to adjust its focus area for larger distances. As demonstrated in Fig. 5, when the model processes amplitude data, it specifically targets the reflections from the object to establish the angle, and this targeted area is dynamically adjusted based on the target’s distance. This indicates the model’s capacity to adapt its analysis to varying distances for effective AOA classification.

*Observation 6:* In contrast to the situation for distance classification, **the combination of amplitude and phase input data results in more focused decision regions in the XAI visualization for AOA**. Based on this result, it can be concluded that both input types should be used to obtain the highest accuracy. Table II, confirms that using both amplitude and phase together yields better AOA classification results at every distance measured than using either amplitude or phase alone. This finding underscores how input selection can already happen before the validation phase through the XAI visualizations.

*Observation 7:* The investigation into the UWB radar system reveals that **a reduced number of antennas can still effectively perform AOA classification**. This conclusion is

drawn from an analysis illustrated in Fig. 5. It was observed that the system only required the first two antennas for accurate angle classification in some cases, such as at a 200cm distance using amplitude data. This finding suggests that two antennas are sufficient for AOA classification under certain conditions. However, the complexity of AOA estimation with UWB radar means that while some antennas may have a lesser role at different distances, they are still utilized. Further supporting this observation, additional training and testing with just two and three antennas showed consistent results with only minor accuracy variations of about  $\pm 2\%$ . This indicates that fewer antennas can indeed be effective for AOA classification. Nonetheless, employing more antennas enhances the system’s robustness, especially over greater distances or in more complex scenarios.

1) *Lessons learned* : Several key lessons have been learned throughout implementing XAI for AOA classification in a UWB radar system. Firstly, the high accuracy of the model in a specific environment indicates that it might be overfitting to the amplitude data of that particular setting, raising concerns about its ability to generalize to new environments. This suggests the need for the model to understand better and incorporate phase information patterns for broader applicability and accurate predictions in varied settings. Secondly, the insights from the XAI approach reveal opportunities for optimizing the CNN architecture used for AOA classification. This includes refining the number and size of variables, which could lead to more efficient training and evaluation processes.

Another insight is balancing complexity and performance in the model design. While a simpler model with fewer antennas can be effective, using more antennas could enhance robustness, especially in complex or changing environments. This highlights the need for a tailored approach in designing radar systems, where the trade-offs between simplicity, accuracy, and adaptability are carefully considered.

## VII. CONCLUSION AND FUTURE WORK

The research paper demonstrated how XAI can be integrated within UWB radar technology. Specifically, this research demonstrates how XAI can enhance the understanding of the workings of CNN models, thereby allowing additional insights and dedicated CNN designs that take these insights into account. The combined evaluation of CNN accuracy with XAI explainability results in more transparent and interpretable algorithms for AI systems on UWB radar. The findings also represent a significant step forward in addressing the challenges posed by AI’s “black box” nature, thereby increasing the understanding and acceptance of AI in critical technological areas. Future research should explore the scalability of the proposed XAI approach in more complex UWB radar scenarios and its applicability across different AI models and domains, further enhancing the reliability and generalizability of AI-driven technologies.

## VIII. ACKNOWLEDGMENTS

This research has been funded by Fonds Wetenschappelijk Onderzoek Vlaanderen (FWO) through grant number G018522N for the FWO PESSO project.

## REFERENCES

- [1] M. Naseri et al. Machine learning-based angle of arrival estimation for ultra-wide band radios. *IEEE Communications Letters*, 26(6):1273–1277, June 2022.
- [2] R. Schmidt. Multiple emitter location and signal parameter estimation. *IEEE Transactions on Antennas and Propagation*, 34(3):276–280, March 1986.
- [3] I. Dotlic, A. Connell, H. Ma, J. Clancy, and M. McLaughlin. Angle of arrival estimation using decawave dw1000 integrated circuits. In *2017 14th Workshop on Positioning, Navigation and Communications (WPNC)*, pages 1–6, Bremen, Germany, March 2017.
- [4] K. Hong, T. Wang, J. Liu, Y. Wang, and Y. Shen. A learning-based aoa estimation method for device-free localization. *IEEE Communications Letters*, 26(6):1264–1267, June 2022.
- [5] B. V. Herbruggen, S. Luchie, R. Berkvens, J. Fontaine, and E. D. Poorter. Impact of cir processing for uwb radar distance estimation with the dw1000 transceiver. In *2023 13th International Conference on Indoor Positioning and Indoor Navigation (IPIN)*, pages 1–7, 2023.
- [6] X. Shang, J. Liu, and J. Li. Multiple object localization and vital sign monitoring using ir-uwb mimo radar. *IEEE Transactions on Aerospace and Electronic Systems*, 56(6):4437–4450, Dec 2020.
- [7] Y. Kilic, H. Wymeersch, A. Meijerink, M. J. Bentum, and W. G. Scanlon. Device-free person detection and ranging in uwb networks. *IEEE Journal of Selected Topics in Signal Processing*, 8(1):43–54, Feb 2014.
- [8] Ledergerber A and D’Andrea R. A multi-static radar network with ultra-wideband radio-equipped devices. *Sensors*, 20(6):1599, 2020.
- [9] Cimdin M, Schmidt SO, and Hellbrück H. Mampi-uwb—multipath-assisted device-free localization with magnitude and phase information with uwb transceivers. *Sensors*, 20(24):7090, 2020.
- [10] S. A. Rane, A. Gaurav, S. Sarkar, J. C. Clement, and H. K. Sardana. Clutter suppression techniques to detect behind the wall static human using uwb radar. In *2016 IEEE International Conference on Recent Trends in Electronics, Information & Communication Technology (RTE-ICT)*, pages 1325–1329, Bangalore, India, May 2016.
- [11] Mankodiya H, Jadav D, Gupta R, Tanwar S, Alharbi A, Tolba A, Neagu B-C, and Raboaca MS. Xai-fall: Explainable ai for fall detection on wearable devices using sequence models and xai techniques. *Mathematics*, 10(12):1990, 2022.
- [12] C. Turetta et al. Towards deep learning-based occupancy detection via wifi sensing in unconstrained environments. In *2023 Design, Automation & Test in Europe Conference & Exhibition (DATE)*, pages 1–6, Antwerp, Belgium, March 2023.
- [13] H. B. Kwon et al. Attention-based lstm for non-contact sleep stage classification using ir-uwb radar. *IEEE Journal of Biomedical and Health Informatics*, 25(10):3844–3853, Oct 2021.
- [14] J. Kulmer et al. Using decawave uwb transceivers for high-accuracy multipath-assisted indoor positioning. In *2017 IEEE International Conference on Communications Workshops (ICC Workshops)*, pages 1239–1245, Paris, France, May 2017.
- [15] M. Cheraghinia, A. Shahid, S. Luchie, G.-J. Gordebeke, O. Caytan, J. Fontaine, B. Van Herbruggen, S. Lemey, and E. De Poorter. A comprehensive overview on uwb radar: Applications, standards, signal processing techniques, datasets, radio chips, trends and future research directions, 2024.
- [16] Ugent industrial iot lab (iiot). Available: <https://www.ugent.be/ea/idlab/en/research/research-infrastructure/industrial-iot-lab.htm>. Accessed: 2024-02-14.
- [17] Sundararajan M, Taly A, and Yan Q. Axiomatic attribution for deep networks. In *International conference on machine learning*, pages 3319–3328, Sydney, Australia, July 2017.